J. Mater. Environ. Sci. 7 (3) (2016) 700-712
ISSN : 2028-2508
CODEN: JMESC

The Computational Study Of The electronic and Optoelectronics Properties of New Materials Based On Thienopyrazine For Application in Dye Solar Cells

M. Bourass [a], A. Touimi Benjelloun [a], M. Benzakour [a], M. Mcharfi [a], M. Hamidi [b], S.M. Bouzzine [b, c], F. Serein-Spirau [d], T. Jarrosson [d], J. P. Lère-Porte [d], J. M. Sotiropoulos [e], M. Bouachrine [f*]

[a] *ECIM/LIMME, Faculty of sciences Dhar El Mahraz, University Sidi Mohamed Ben Abdallah, Fez, Morocco.*
[b] *Equipe d'Electrochimie et Environnement, Faculté des Sciences et Techniques, Errachidia, University Moulay Ismaïl, Meknes, Morocco*
[b, c] *Centre Régional des Métiers d'Education et de Formation, BP 8, Errachidia, University Moulay Ismaïl, Meknes, Morocco*
[d] *Hétérochimie Moléculaire et Macromoléculaire, UMR CNRS 5076, Ecole Nationale Supérieure de Chimie de Montpellier, Montpellier, France*
[e] *Université de Pau et des Pays de l'Adour, UMR5254 – IPREM, Equipe Chimie-Physique, Hélioparc –PAU, France.*
[f] *ESTM, (LASMAR), University Moulay Ismaïl, Meknes, Morocco*

Received 31 July 2015, Revised 23 Dec 2015, Accepted 04 January 2016
**For correspondence: Email:* bouachrine@gmail.com *(M. Bouachrine); Phone:* +212 5 35 73 31 71, +212 6 60 73 69 21*; Fax:* +212 5 35 73 31 71

Abstract

To understand the importance of the organic material of type donor-π-acceptor dyes (D-π-A), used for dye-sensitized solar cells (DSSCs), we present in this paper the result of six compounds based on thienopyrazine (D1-D6) studied by density functional theory (DFT) and time dependent DFT (TD-DFT) approaches to shed light on how the π-conjugation order influence the performance of the dyes. The electron acceptor (anchoring) group was 2-cyanoacrylic acid for all dyes whereas the electron-donor unit varied and the influence was investigated. The theoretical results have shown that TD-DFT calculations using the Coulomb attenuating method CAM-B3LYP with the polarized split-valence 6-31G (d, p) basis sets and the polarizable continuum model (PCM) were reasonably capable of predicting the excitation energies, the absorption and the emission spectra of the dyes. The study of structural, electronic and optical properties for these dyes could help to design more efficient functional photovoltaic organic materials. Key parameters in close connection with the short–circuit current density (Jsc), including light harvesting efficiency (LHE), injection driving force (ΔGinject) and total reorganization energy (ltotal), were discussed.

Keywords: Dye-sensitized Solar Cells; Thienopyrazine derivatives; DFT; Photovoltaic; Optoelectronic properties.

1. Introduction

Organic materials based on π-conjugated molecules have been drawing broad research attention due to their practical applications in device technology [1-3], such as solar cells [4, 5], light-emitting diodes (LEDs) [6-11], and field-effect transistors (FETs) [12-17]. In the field of organic solar cells, conjugated molecules are a subject

of an increasing interest in recent years due to their advantages of low cost, light weight, process ability and potential to make flexible photovoltaic devices in comparison with the traditional silicon-based solar cells.
One class of these devices that received great attention was Dye Sensitized Solar Cells (DSSCs) that have attracted ever-increasing attention in scientific research and in practical applications since the first report by O'Regan and Grätzel in 1991, because of its potential advantages, such as low cost and highly efficient conversion of sunlight into electricity [18, 19]. In particular, these DSSC are composed of a wide band gap semi-conductor (typically TiO_2) sensitized with molecular dyes, able to capture light in the visible region of the spectrum, and a redox electrolyte (typically Iodide/triiodide I^-/I_3^-) [20, 21]. In DSSCs, incoming light causes electronic excitations of the dye sensitizers leading to electron injection to the conduction band of nanocrystalline metal oxide, then, the dyes regain electrons from the redox couple in an electrolyte solution [22]. In general, a power conversion efficiency dye sensitizer has the following characteristics: the highest occupied molecular orbital (HOMO) energy must be located below the HOMO energy of electrolyte to accept the electron from a redox electrolyte pair (I^-/I_3^-), the lowest unoccupied molecular orbital (LUMO) should have a higher energy than that of the conduction band of semi-conductor (TiO_2).
The most extensively studied organic dyes usually adopt the donor–π space–acceptor (D-π-A) structural motif, which exhibit several advantages: high molar extinction coefficients, low cost of production, and an extraordinary diversity [23]. In this structure, the intra-molecular charge transfer (ICT) from D to A at the photo-excitation will inject the photoelectron into the conduction band of the semiconductor through the electron accepting group at the anchoring unit. By changing the electron donor, acceptor, and/or –π spacer group, the HOMO and LUMO energy levels are affected [24]. Thus, many researchers have conducted for the objective to develop new π-conjugated materials based on with donor-acceptor-donor (D-π-D) structure, especially compounds containing thienopyrazine have been the subject of several studies and numerous works [25, 26]. However, the electronic and photovoltaic properties of Dye Sensitized Solar Cells (DSSCs) based on these materials are rarely discussed and studied. In this context, we present herein theoretical study of the structural and optoelectronic properties of new designed donor and acceptor systems based on thienopyrazine (D1, D2, D3, D4, D5 and D6) shown in Figure 1.

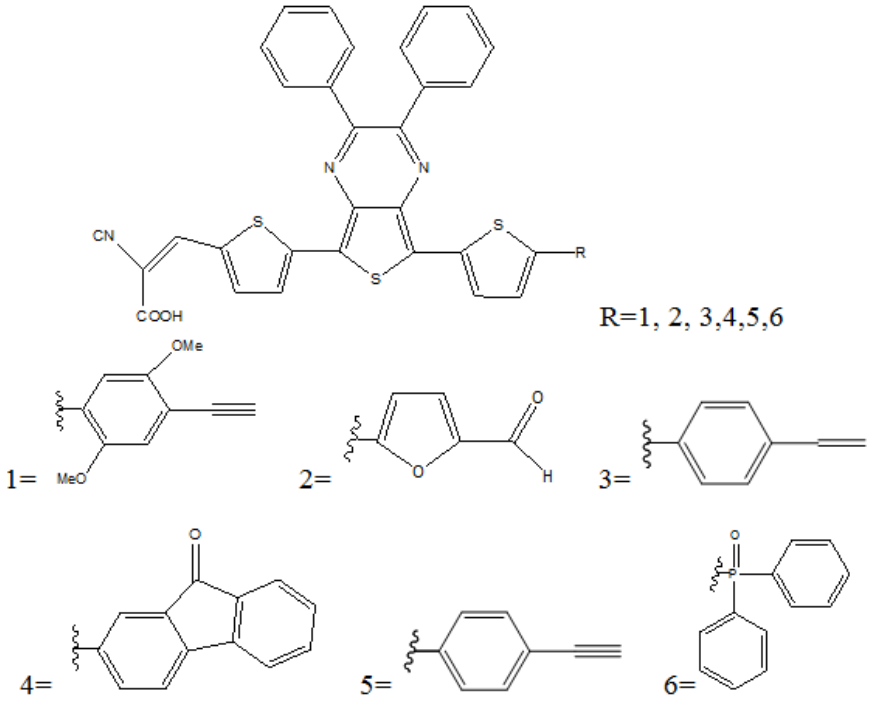

Figure 1: Chemical structure of study compounds Di (i =1 to 6)

2. **Theoretical methodology**

All molecular calculations were performed in the gas phase using Density Functional Theory (DFT) using the B3LYP (Becke three-parameter Lee–Yang–Parr) exchange correlation functional [27]. The basis set 6-31 G (d, p) was used for all atoms. All the optimizations were done without constraint on dihedral angles. In a recent work, Tretiak and Magyar [28] have demonstrated in a series of D-π-A systems that a good description of the charge transfer states can be achieved when a large fraction of Hartree-Fock (HF) exchange is used. A newly designed, functional, the long rang Coulomb attenuating method (CAM-B3LYP) considered long-range interactions by comprising 19% of HF and 81% of B88 exchange at short-range and 65% of HF and 35% of B88 at long-range [29]. Furthermore, The CAM-B3LYP has been applied and was reasonably capable of predicting the excitation energies and the absorption spectra of the D-π-A molecules [30-33]. Therefore, the vertical excitation energy and electronic absorption spectra were simulated using the TD-CAM-B3LYP method in this work. The inclusion of the solvent effect on theoretical calculations is important when seeking to reproduce or predict the experimental spectra with a reasonable accuracy. Polarizable continuum model (PCM) [34] has emerged in the last two decades as the most effective tools to treat bulk solvent effects for both the ground and excited-states. In this paper, the integral equation formalism polarizable continuum model (IEF-PCM) [35-36] was chosen in excitation energy calculations. The ground state energies and oscillator strengths were investigated using TD-DFT calculations on the fully DFT optimized geometries. The calculations were carried out using the Gaussian 09 program [37].

3. **Results and discussion**

3.1. Ground state geometry

The best predicted theoretical results of molecular geometries from the DFT method with the hybrid B3LYP function can be justified by comparing with the experimental results reported in the literature. To verify the theoretical geometry, it was found in other works [38, 39] that the experimental X-ray diffraction data for EDOT–thienopyrazine–EDOT is in excellent agreement with the theoretical result obtained by using DFT-optimized geometries with the hybrid B3LYP function. All the molecular geometries have been calculated with the hybrid B3LYP function combined with 6-31G (d, p) basis sets using Gaussian 09 program. The optimized structures of all studied compounds are illustrated in Figure 2. It reveals that the π-electron delocalization between different aromatic units is clear. The results of the optimized structures for all studied compounds show that they have similar conformation (quasi-flat conformation).

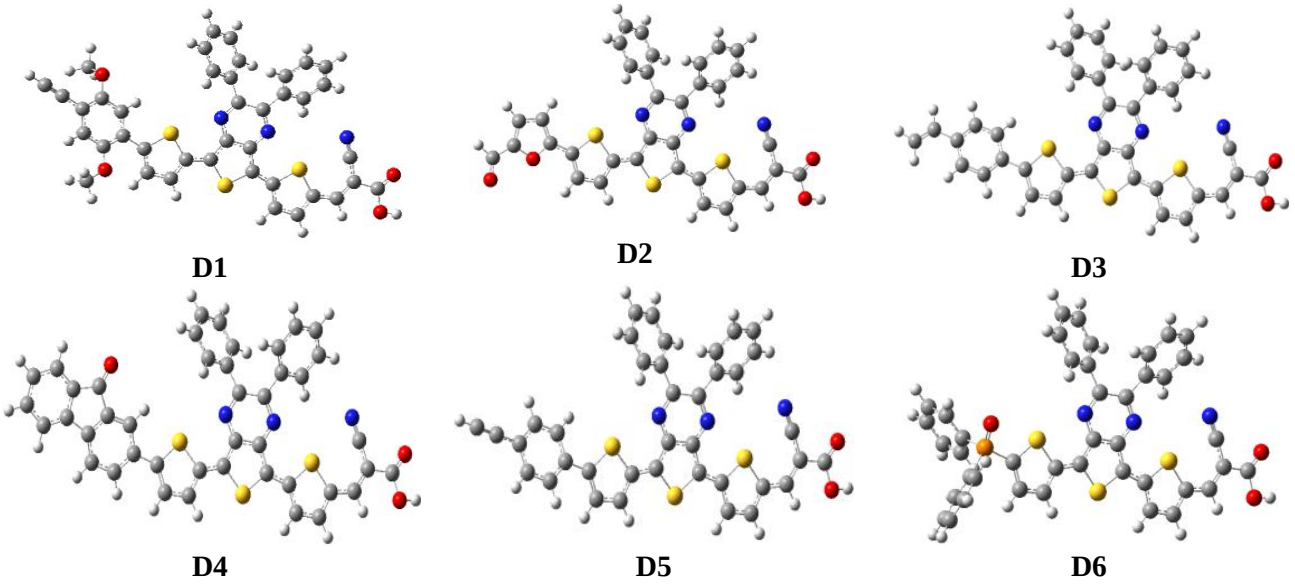

Figure 2: Optimized geometries obtained by B3LYP/6-31G (d, p) of the studied molecules.

The main optimized ground and excited state geometry parameters of six compounds (D1, D2, D3, D4, D5 and D6) are given in Table 1. In the systems D-π-A, the π-spacer is used as the bridge of intramolecular charge transfer (ICT), therefore, the bridge bonds between A and π-spacer, and D and π-spacer tike an account of the interaction among themselves. Herein, the bridge bonds between D and π-spacer and A and π-spacer were marked as L_{B1} and L_{B2} respectively. The shorter length of the bridge bonds favored the ICT within the D- π-A molecules. Table 1 shows that L_{B1} of D1, D2, D3, D4, D5 and D6 in the ground state (S_0) are 1.463, 1.435, 1.462, 1.463, 1.462 and 1.818 Å respectively, from the length range of C–C to C=C, of which L_{B1} shows more C=C features. These bond lengths are sorted in the order of D2>D3=D5>D1=D4>D6, which presents the intensity of interaction between thiophene-thienopyrazine-thiophene based bridge and donor groups. However, the abnormal L_{B1} of D2 and D6 results from the intense and lowest π-conjugated effect respectively. For all the molecules, L_{B2} does not change significantly. It implies the interaction between A and π-spacer is hardly influenced by D-π interactions.

In order to state the molecular planarity clearly, two parameters were introduced: Φ_1, Φ_2. Here, Φ_1 is the torsional angle between D and π-spacer, Φ_2 is the torsional angle between A and π-spacer. Table 1 shows that Φ_2 is similar for all molecules in the ground state, while Φ_1 for D1, D2, D3, D4, D5 and D6 are 19.72°, 0.78°, 22.19°, 22.04° , 22.71° and 41.37° respectively (Tab. 1), which indicates a tendency that close to coplanarity except D1, D3, D4, D5and D6 due probably to the steric effects of donor groups. It indicates the Φ_1 of D6 is abnormally great, which may be caused by the associated influence of diphenylphosphane conjugation and thiophene steric effects. Therefore, the introduction of diphenylphosphane is disadvantageous to the molecular planarity and conjugated effect. On the other hand the values of the bond lengths and torsional angle obtained for these studied molecules in the excited state (S_1) are quasi-similar in comparison with those in the ground state (S_0).

Table 1: Optimized selected bond lengthsand bond angles of the studied molecules obtained by B3LYP/6-31G (d, p) level.

	S_0				S_1			
Compounds	L_{B1}	L_{B2}	Φ_1	Φ_2	L_{B1}	L_{B2}	Φ_1	Φ_2
D1	1.463	1.421	19.72	2.77	1.449	1.411	14.17	3.41
D2	1.435	1.423	0.78	2.95	1.425	1.413	0.56	3.98
D3	1.462	1.421	22.19	2.85	1.449	1.411	10.07	3.67
D4	1.463	1.422	22.04	2.82	1.451	1.411	11.61	3.34
D5	1.462	1.422	22.71	2.84	1.452	1.412	12.68	3.53
D6	1.818	1.422	41.37	2.76	1.810	1.412	42.23	3.50

3.2. Frontier molecular orbitals

Generally for enhance the light harvesting efficiency of DSSCs, the choice of the appropriate donor and acceptor spacer are essential, so the strong group donating of electron give a high E_{HOMO} energy level, while the strong group accepting of electron causes of a low E_{LUMO} energy level. Therefore, we calculated the frontier orbital energy gaps between HOMO and LUMO of six compounds (D1, D2, D3, D4, D5 and D6) which are illustrated in Figure 3. The calculation by using B3LYP/6-31G (d, p) of the highest occupied and lowest unoccupied molecular orbital's get approximate HOMO/LUMO energies of -5.025/-3.057 eV for D1, -5.276/-3.293 eV for D2, -5.091/-3.099 eV for D3, -5.139/-3.124 eV for D4, -5.155/ -3.140 eV for D5 and -3.140/ -3.159 eV for D6, corresponding to energy gaps of 1.968 eV for D1, 1.983 eV for D2, 1.992 eV for D3, 2.015 eV for D4, 2.015 eV for D5 and 2.171eV for D6. The increased π-conjugated system of six compounds (D1, D2, D3, D4, D5, and D6) make the energy of HOMO and LUMO stabilized and the energy gaps between HOMO and LUMO decrease, which would make the organic photovoltaic (OPV) spectra red shifted. We can remark that the energy gap increases when going from D1 to D6 in the following order D1<D2< D3 <D4<D5<D6. Finally, the energy gap of D1, D2 and D3 are much smaller than that of the other compounds.

This probably due to the effect of π-conjugation of donor units with the π-bridge, this leads to the increase of charge transfer from the donor unit (R) to the acceptor moiety.

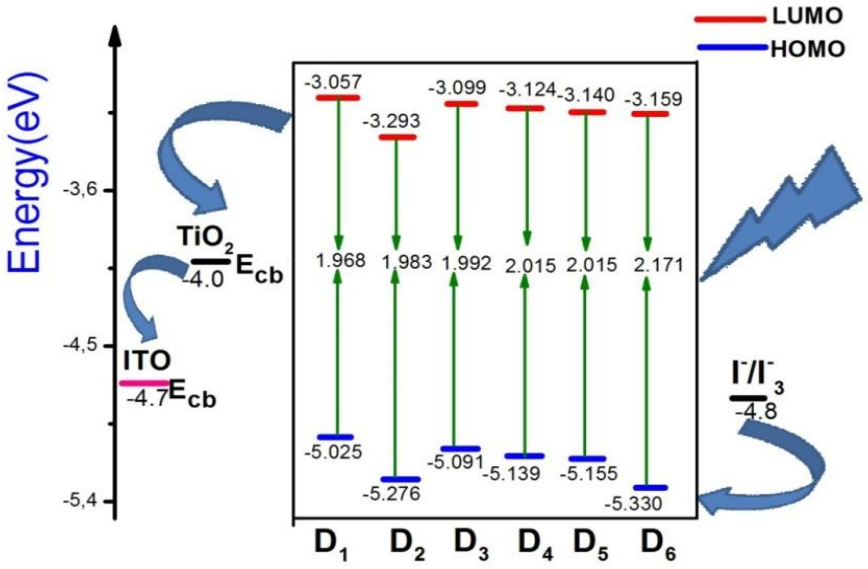

Figure 3: Schematic energy diagram of all dyes, TiO_2 and electrolyte (I^-/I^-_3)

It is found that increasing more π-conjugated donor units in D1, D2 and D3 gradually decreased the Eg for dyes with long conjugation length D1–D3, it was shown clearly that inserting the group cyclic which contain or attached with a hetero atom ring in the electron-donor group (oxygen in the dyes D1 and D3 respectively and sulfur in the dye D2) increases the Eg. This finding was supported by the researcher's previous report, which indicated that the phenylene unit was not suitable for the extension of the conjugation system [40]. Compounds D1, D2 and D3 with this lowest energy gap are expected to have most outstanding photophysical properties.
The electron spatial distribution of the highest occupied molecular orbital (HOMO), and lowest unoccupied molecular orbital (LUMO) in the ground state of all compounds in the gas phase is plotted (Figure 4). The distributions of HOMO levels have difference. The HOMOs of D1, D2 and D3 are almost delocalized over the whole molecule, but that of D4, D5 and D6 mainly distributes in π-bridge and only a little part of it is localized in the acceptor unit. While the LUMO orbital possesses for six compounds have a larger contribution of the π-bridge groups (thiophene-thienopyrazine-thiophene) and near the carboxyl groups is observed of all compounds, which is called anchoring or acceptor group. The results show that electron transfer from acceptor chromophor via thiophene-thienopyrazine-thiophene to carboxyl anchoring group takes place during the excitation process of D1, D2, D3, D4, D5 and D6. The electronic transition of D1, D2, D3, D4, D5 and D6 indicates that when an electron at ground state is excited by a photon from the sunlight, electron would transfer from the donor group (D1, D2, D3, D4, D5 or D6) to TiO_2 electrode. Because D1, D2, D3, D4, D5 and D6 are anchored onto the TiO_2 surface through carboxylic acid, an electron injection process will be facilitated as the molecule is excited.

3.3. Photovoltaic properties

The HOMO and the LUMO energy levels of the donor and acceptor components are very important factors to determine whether the effective charge transfer will happen between the donors (Di) and acceptor (TiO_2). To evaluate the possibilities of electron transfer from the excited studied molecules to the conductive band of the acceptor TiO_2, the HOMO and LUMO levels were compared (Figure 3). It is important to note that the LUMO levels of the dyes are higher than that of the conduction band of TiO_2 (-4.0 eV, [41]). The LUMO energy levels of all dyes are much higher than that of TiO_2 conduction band edge suggesting that the photo-excited electron transfer from Di to TiO_2 may be sufficiently efficient to be useful in photovoltaic devices.

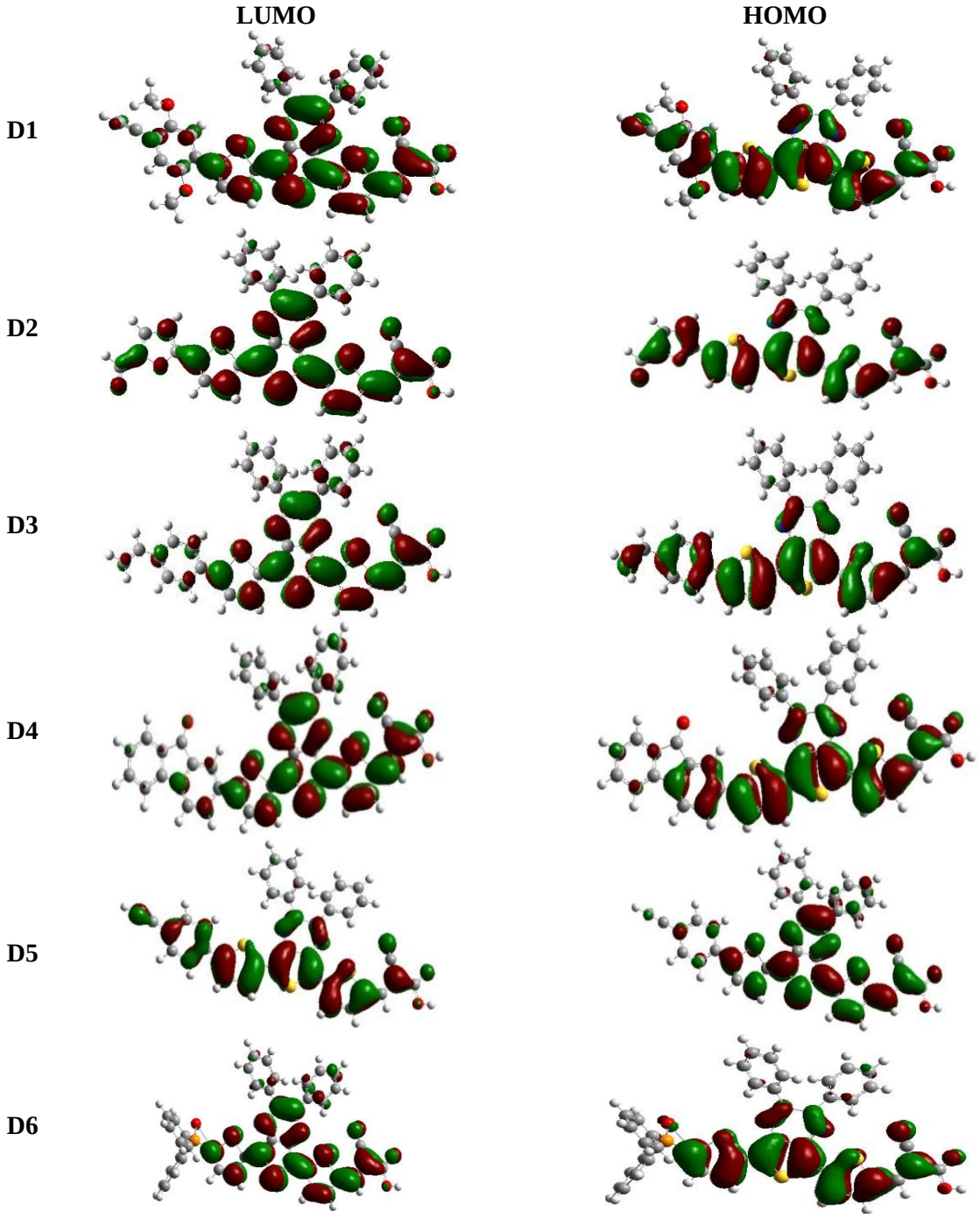

Figure 4: The contour plots of HOMO and LUMO orbital's of the studied compounds Di (i=1 to 6).

The power conversion efficiency (η) was calculated according to the Eq. 1:

$$\eta = FF \frac{V_{oc} J_{sc}}{P_{inc.}} \quad (1)$$

where $P_{inc.}$is the incident power density, *Jsc* is the short-circuit current, Voc is the open-circuit voltage, and *FF* denotes the fill factor.

To analyze the relationship between V_{OC} and E_{LUMO} of the dyes based on electron injection (In DSSCs) from LUMO to the conduction band of semiconductor TiO_2 (E_{CB}), the energy relationship can be expressed [42]:

$$Voc = E_{LUMO} - E_{CB} \quad (2)$$

The obtained values Voc of the studied dyes calculated according to the Eq. 2 range from 0.707 eV to 0.943 eV of TiO_2 (Tab. 2) these values are sufficient for a possible efficient electron injection.

Table 2: Estimated electrochemical parameters for all dyes

dyes	P.I (eV)	A.E(eV)	λ_h	λ_e	λ_{total}	E_{00}	E^{dyes}	E^{dyes*}	ΔG_{inject}	LHE	V_{OC}
D1	5.887	2.186	0.22	0.27	0.49	2.0963	5.025	2.9287	-1.0713	0.95	0.943
D2	6.181	2.409	0.22	0.14	0.36	2.1215	5.276	3.1545	-0.8455	0.94	0.707
D3	5.970	2.214	0.22	0.27	0.49	2.1183	5.091	2.9727	-1.0273	0.94	0.901
D4	5.991	2.267	0.23	0.25	0.48	2.1334	5.138	3.0046	-0.9954	0.95	0.876
D5	6.043	2.253	0.22	0.27	0.49	2.1362	5.155	3.0188	-0.9812	0.94	0.860
D6	6.221	2.292	0.30	0.36	0.66	2.2618	5.330	3.0682	-0.9318	0.91	0.841

3.3.1. Theoretical background

Generally, in DSSCs, the short–circuit current density *Jsc* is determined as:

$$J_{SC} = \int_{\lambda} LHE(\lambda)\, \Phi_{inject}\ \eta_{collect}\ d\lambda \qquad (3)$$

where the LHE(λ) is the light harvesting efficiency at a given wavelength, Φ_{inject} is the electron injection efficiency, and $\eta_{collect}$ is the charge collection efficiency. As a result, to understand the relationship between the *Jsc* and η theoretically, we investigated the *LHE*, Φ_{inject} and total reorganization energy (λ_{total}). As mentioned in Eq. 3, the large LHE lead to high *Jsc*, therefore enhance the efficient of DSSCs. The LHE can be expressed as [43]:

$$\mathrm{LHE} = 1 - 10^{-f} \qquad (4)$$

where *f* is the oscillating strength of the dyes associate to the absorption energy (E_{00}).

Based on Eq. 3, the large Φ_{inject} lead to a high *Jsc*, in which the Φ_{inject} is related to the driving force (ΔG^{inject}) of the electron injection from the photo-induced excited states of organic dyes to semiconductor surface. Generally, the larger ΔG^{inject}, the larger Φ_{inject}, and it (in eV) can be expressed as [51]:

$$\Delta G^{inject} = E^{idye*} - E_{CB} \qquad (5)$$

where $E^{dye}*$ present the oxidation potential energy of the dye in the excited state and E_{CB} present the reduction potential of the conduction band of semi-conductor (TiO_2). In this work we will use the E_{CB} = –4.0 eV for TiO_2 [41], for the reason that it is very used for the some works [44-49], and the E^{dye*} can be estimated by the following equation [46-50]:

$$E^{dye*} = E^{dye} - E_{00} \qquad (6)$$

where E^{dye} present the energy of oxidation potential for ours dye in the ground state, whereas E_{00} is the energy of electronic vertical transition corresponding to λ_{max}.

In order to enhance the *Jsc* and as mentioned in Eq. 3, the small total reorganization energy (λ_{total}) lead to a high *Jsc* , in which the λ_{total} is the sum of reorganization energy of the hole and electron. Therefore, in order to enhance the LHE and Φ_{inject} as well as decreasing the reorganization energy (λ_{total}). So we computed the hole and the electron reorganization energy (λ_h and λ_e) according to the following formula [51]:

$$\lambda_i = [E_0^{\pm} - E_{\pm}^{\pm}] - [E_{\pm}^{0} - E_0] \qquad (7)$$

Where $E_0^{\pm}$ is the energy of the cation or anion calculated with the optimized structure of the neutral molecule, $E_{\pm}^{\pm}$ is the energy of the cation or anion calculated with the optimized cation or anion structure, $E_{\pm}^{0}$ is the energy of the neutral molecule calculated at the cationic or anionic state, and the E_0 is the energy of the neutral molecule at ground state.

as discussed previously and as mentioned in Eq. 3 we remark that the light harvesting ability (LHE) and the electronic injection free energy (ΔG^{inject}) are the two main influencing factors on *Jsc* (Eq. 3) and therefore in efficiency of the organic dyes. The LHE is considered as a very important factor for the organic dyes in which we could appreciate the role of dyes in the DSSC, i.e. absorbing photons and injecting photo-excited electrons to

the conduction band of the semi–conductor (TiO_2). In the order to know and to give an intuitional impression to how the influencing of donor spacer of the LHE, we simulated the UV/Vis absorption spectra of the six dyes. We find that as the donor spacer changing, the oscillator strengths were changed slightly. As shown in Table 2**,** the LHE of the dyes fall within the range: 0.91–0.95. The LHE values for the dyes are in narrow ranges. This means that all the dyes will give similar photocurrent**.**

As mentioned above, for enhancing the value of *Jsc* another factor was introduced which is the electronic injection free energy ΔG^{inject}. The details calculation of the ΔG^{inject} has been described in Eq. 5. The ground state oxidation potential energy is related to ionization potential energy according the Koopman's theorem [52]. Furthermore the E^{dye} can be estimated as negative E_{HOMO} [53] and E^{dye*} is calculated based on Eq. 6. Through the results shown in Table 3, we observe that the electron donor significantly influences on E^{dye*}. We remark also that for all studied dyes, ΔG^{inject} is negative, this reveal that the electron injection process is spontaneous, and the calculated ΔG^{inject} for these six dyes is decreased in the following order of D2>D6>D5>D4>D3>D1**.** Among these six dyes, we observe that the dye D2, D6, D5 and D4 have the larger ΔG^{inject}, this maybe is due to the influencing of the donor spacer from ours dyes**.** As a results, and based just from LHE and ΔG^{inject} related to *Jsc* , we could conclude that the cell containing the dye D2, D6, D5 and D6 should have the highest *Jsc* due to its relative large LHE and injection driving force compared to the dyes D1, D3.

In other side the reorganization energy λ_{total} is also important factor influencing in the kinetics of electron injection. Therefore for analyze the relationship between the electronic structure and the *Jsc* it is necessary to calculate the reorganization energy (λ_{total}). As mentioned previously, the small λ_{total} which contains the hole and electron reorganization energy increase the *Jsc*. Through the Table 2, we remark that the calculated λ_{total} of all dyes are increased in the following order: D2<D4<D1=D3=D5<D6. These results show that dyes D2 and D4 have the smallest total reorganization energy whereas the dyes D6 have the largest. Furthermore, and for high efficient DSSCs, it is important to realize the balanced of both holes and electrons reorganization energy, therefore, the more balanced reorganization energy of hole and electron obtained, the more higher luminous efficiency will have [44, 52]. From the table 2 we remark that the differences between λ_h and λ_e of six dyes D1–D6 are 0.5, 0.8, 0.5, 0.2, 0.5 and 0.6 eV respectively. Thus, the weak difference between both holes and electrons reorganization energy of all dyes indicate that these six dyes are more balanced transport**.** As a result, we could predict that these six dyes are favorable candidates from DSSCs and can exhibit a high efficiency.

3.3.2. Ionization potentials (IP) and electron affinities (EA)

The adequate and balanced transport of both injected electrons and holes is main factor to determine the performance of electronic devices. For estimate the energy barrier for the injection of both holes and electrons into the dye, calculated by the DFT of the ionization potential (IP) and electron affinity (EA) are necessary. Table 2 shows the ionization potential and electrons affinities. One general challenge for the application in the LEDs is the achievement of high electron affinity (n-type) conjugated molecule for improving electron injection/transport and low ionization potential (p-type) conjugated molecule for better hole injection/transport in organic electronic devices. The energies required to inject holes in the dyes for six D1, D2, D3, D4, D5 and D6 are: 5.887, 6.181, 5.97, 5.991, 6.043 and 6.221eV, respectively, which are all lower, and this is adequate to the analysis results for HOMO energy.

3.4. Absorption and emission properties

The predicted of the Excitation energies and oscillator strengths by using the CAM-B3LYP is good agreement with the experimental results [53,54] than is found for B3LYP, because The CAM-(Coulomb-attenuating method) B3LYP was also examined for taking account of the long-range corrections for describing the long π-conjugation [55], in other side the results shown in the Tab. 3 illustrate that the excitation energy (HOMO to LUMO) values (Gap opt.) obtained by TD-DFT/CAM-B3LYP /6-31G (d, p) level in chloroform solvent is quasi-agree with the values of gap energy obtained by DFT/B3LYP/6-31G (d, p) level, therefore the CAM-B3LYP functional is very well for predicting the Excitation energies (Eg opt.) (HOMO to LUMO). The

calculated by using the TD- CAM-B3LYP functional of six dyes in vacuo and in chloroform solvent for predicting the Excitation energies and oscillator strengths are listed in Table 3 and Table 4 respectively.

Table 3: Excitation absorption energy values (ΔE) for six dyes obtained by TD-DFT level in vacuo and in chloroform solvent.

Dye	Gap opt (eV)			Gap (eV)
	TDDFT/B3LYP	TDDFT/CAM-B3LYP		DFT/B3LYP
	vacuo	Vacuo	chloroform	
D1	1.82	2.10	1.98	1.97
D2	1.85	2.12	2.01	1.98
D3	1.84	2.12	2.00	1.99
D4	1.85	2.13	2.01	2.02
D5	1.86	2.14	2.02	2.02
D6	2.00	2.26	2.16	2.17

The TD/CAM-B3LYP/6-31G (d, p) method was employed to simulate the optical property of the dyes. The computed vertical excited singlet states, transition energies and oscillating strength of all dyes in vacuo and chloroform solvent media are tabulated in Tab. 4. The first vertical excitation energies (ΔE_{excit}) of the dyes are in decreasing order: D6>D5>D4>D2>D3>D1. ΔE_{excit} for all dyes is lowering from vacuo to solvent phase. The transition energy in vacuo is almost equal to in chloroform. The transition characters related to the excitation in vacuo and in chloroform are similar. According to the transition character, most of the dyes show the HOMO→LUMO transition (in solvent) as the first singlet excitation. The major contribution of the transition characters in vacuo differs from those solvent due to the effect of polar environment on the electronic energy level. The maximum (λ_{max}) wavelengths for UV–vis absorption spectra of all dyes simulated in various media are shown in Tab.4. The calculated λ_{max} in chloroform and in vacuo are not different (λ_{max}=34 nm). The spectra, in general, are characterized by one dominant, low-energy transition with large oscillator strength followed by a second, high-energy transition (or series of transitions) with smaller oscillator strengths.

The absorption wavelengths increase progressively with the increasing of conjugation lengths. As shown in Table 5 and Figure 5, the absorption wavelengths of D1, D2, D3, D4, D5 and D6 in vacuo and in chloroform solvent are (591.46, 584.40, 585.30, 581.15, 580.40 and 548.16) and (625.38, 618.01, 620.04, 615.49, 613.46 and 574.33) respectively, indicating all molecules have only one band in the Visible region (λ_{abs}> 400 nm) and D1 has the maximum absorbent wavelength.

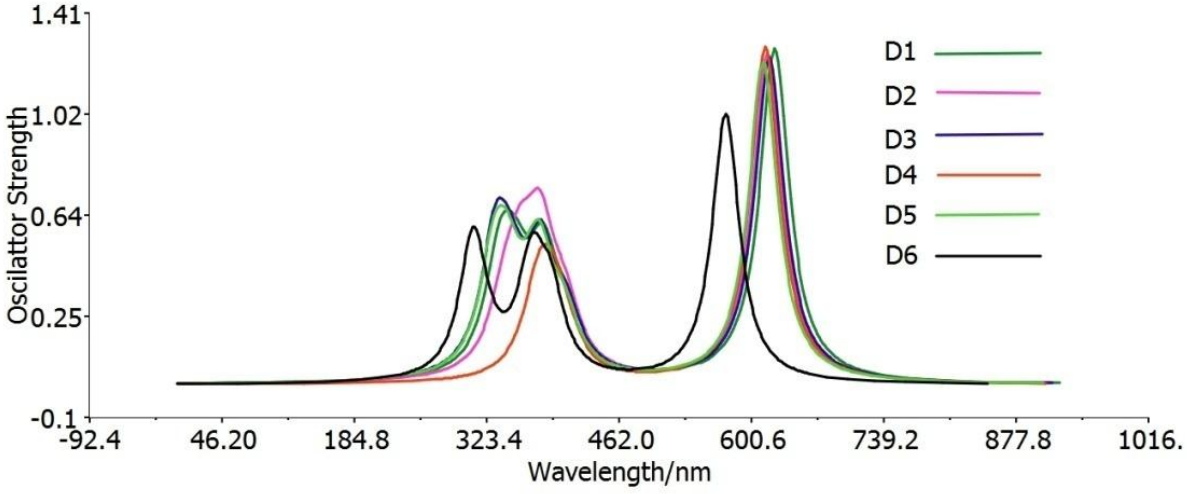

Figure 5: Simulated UV-visible optical absorption spectra of the title compounds with the calculated data at the TDDFT/CAM-B3LYP/6-31G(d,p) level in chloroform solvent.

Table 4: The vertical singlet states, transition character and oscillating strength of the absorption bands in UV–vis region for all dyes computed at the TDDFT/CAM-B3LYP/6-31G (d, p) level.

Dye	Energies ΔE (eV)		ʎ absorption		Transition characters[a]		*f*	
	Vacuo	Chloroform	Vacuo	Chloroform	Vacuo	Chloroform	Vacuo	Chloroform
D1	2.09	1.98	591.46	625.38	H → L (69%)	H → L (69%)	1.0923	1.2732
	3.11	3.02	398.44	410.18	H → L+1 (50%)	H → L+1 (53%)	0.1749	0.1685
	3.26	3.23	380.21	383.47	H-1 → L (41%)	H-1 → L (41%)	0.3474	0.4179
	3.40	3.42	364.66	361.61	H-7 → L (33%)	H- 8 → L (34%)	0.0042	0.0088
	3.57	3.50	347.08	354.14	H-2 → L (47%)	H-2 → L (49%)	0.1925	0.2565
	3.70	3.67	335.31	337.86	H → L+2 (50%)	H → L+2 (52%)	0.3701	0.4051
D2	2.12	2.01	584.40	618.01	H → L (69%)	H → L (69%)	1.0513	1.2540
	3.14	3.05	395.02	406.27	H-1 → L (52%)	H → L+1 (48%)	0.2238	0.2142
	3.29	3.26	376.75	380.40	H → L+1 (46%)	H → L+1 (40%)	0.3532	0.4763
	3.40	3.42	364.73	362.53	H -6 → L (38%)	H -6 → L (36%)	0.0080	0.0541
	3.54	3.46	350.53	358.12	H → L+2 (57%)	H → L+2 (49%)	0.3463	0.2819
	3.66	3.63	338.75	341.95	H-2 → L (58%)	H-2 → L (54%)	0.1583	0.2157
D3	2.12	2.00	585.30	620.04	H → L (69%)	H → L (69%)	1.0564	1.2416
	3.13	3.04	395.74	407.99	H → L+1(52%)	H → L+1(55%)	0.1888	0.1837
	3.29	3.27	377.35	380.69	H-1 → L (44%)	H-1 → L (44%)	0.3589	0.4331
	3.40	3.43	364.16	361.06	H-6 → L (43%)	H-7 → L (40%)	0.0065	0.0073
	3.63	3.55	341.90	348.94	H-2 → L (50%)	H-2 → L (49%)	0.1813	0.2530
	3.75	3.72	330.65	332.93	H → L+2 (52%)	H → L+2 (53%)	0.4313	0.4678
D4	2.13	2.01	581.15	615.49	H → L (69%)	H → L (69%)	1.1148	1.2817
	3.12	3.03	398.01	409.13	H -1 → L (43%)	H → L+1 (40%)	0.1022	0.0909
	3.22	3.15	384.73	393.01	H → L+2 (49%)	H → L+2 (49%)	0.2678	0.2699
	3.31	3.28	374.83	377.82	H-1 → L (40%)	H-1 → L (40%)	0.2023	0.2972
	3.39	3.43	365.73	361.74	H-9 → L+1 (61%)	H-6 → L (40%)	0.0010	0.0166
	3.40	3.47	365.01	357.26	H-6 → L (39%)	H-10 → L (60%)	0.0189	0.0003
D5	2.14	2.02	580.40	613.46	H → L (69%)	H → L (69%)	1.0411	1.2234
	3.15	3.06	393.69	405.05	H-1 → L (51%)	H → L+1 (55%)	0.1894	0.1858
	3.30	3.28	375.39	378.27	H -1 → L (44%)	H -1 → L (46%)	0.3516	0.4348
	3.40	3.43	364.43	361.41	H-6 → L (43%)	H-6 → L (40%)	0.0095	0.0083
	3.65	3.58	339.74	346.22	H-2 → L (49%)	H-2 → L (48%)	0.2049	0.2820
	3.76	3.74	329.42	331.53	H → L+2 (49%)	H → L+2 (49%)	0.3748	0.3939
D6	2.26	2.16	548.16	574.33	H → L (69%)	H → L (69%)	0.8707	1.0239
	3.23	3.17	383.99	391.05	H-1 → L (49%)	H-1 → L (51%)	0.2536	0.2713
	3.36	3.34	369.52	371.16	H-10 → L (34%)	H -1 → L (48%)	0.1505	0.3935
	3.40	3.41	364.30	363.12	H → L+1 (44%)	H-10 → L (38%)	0.1664	0.0208
	3.88	3.85	319.15	322.33	H-2 → L (64%)	H-2 → L (61%)	0.0042	0.0341
	4.04	4.00	307.09	309.64	H → L+2 (54%)	H → L+2 (57%)	0.4690	0.5322

[a] Major contribution to the transitions are in parenthesis.

In order to study the emission photoluminescence properties of the studied compounds Di (i=1 to 6), the adiabatic emission spectra were obtained using the optimized geometry of the first excited singlet state at the TDDFT/CAMB3LYP/ 6-31G (d, p) level in chloroform. The emission spectra data of the compounds recorded in chloroform are collected in Table 5.

Table 5: Emission spectra data for all dyes obtained with PCM-CAM-B3LYP/6-31 G (d. p).

	D1	D2	D3	D4	D5	D6
λmax emi (nm)	805.02	794.65	801.53	793.82	790.72	727.01
λmax abs (nm)	625.38	618.01	620.04	615.49	613.46	574.33
SS (nm)	179.64	176.64	181.49	178.33	177.26	152.68

The normalized photoluminescence (PL) spectrum of the studied compounds shows a maximum at 805.02 nm for D1, 794.65 nm for D2, 801.53 nm for D3, 793.82 nm for D4, 790.72 nm for D5 and 727.01 nm for D6 (Tab. 5). This could be regarded as an electron transition process that is the reverse of the absorption corresponding mainly to the LUMO-HOMO electron transition configuration. Moreover, the observed red-shifted emission of the PL spectra is in reasonable agreement with the obtained results of absorption. We can also note that relatively high values of Stocks Shift (SS) are obtained from all dyes D1 (179.64 nm), D2 (176.64), D3 (181.49 nm), D4 (178.33 nm), D5 (177.26 nm) and D6 (152.68 nm) (Tab. 5). In fact, the Stocks Shift, which is defined as the difference between the absorption and emission maximums (EVA-EVE), is usually related to the band widths of both absorption and emission bands [56, 57].

Conclusions

In this study, we have used the DFT/B3LYP method to investigate theoretical analysis of the geometries and electronic properties of some thienopyrazine-derivatives in alternate donor-π-acceptor structure. The modification of chemical structures can greatly modulate and improve the electronic and optical properties of pristine studied materials. The electronic properties of new conjugated materials based on thienopyrazine and heterocyclic compounds and different acceptor moieties have been computed by using 6-31G (d, p) basis set at a density functional B3LYP level, in order to guide the synthesis of novel materials with specific electronic properties. The concluding remarks are:

- The predicted band gaps by using DFT-B3LYP/6-31G (d, p) are in the range of 1.97– 2.17 eV, knowing that the small band gap due to the increasing the displacement the electron between donor and acceptor spacer is very easy.
- The LUMO energy levels of all dyes are much higher than that of TiO_2 conduction band edge, suggesting that the photo-excited electron transfer from Di to TiO_2 may be sufficiently efficient to be useful in photovoltaic devices.
- The obtained values Voc range from 0.707 eV to 0.943 eV of TiO_2. These values are sufficient for a possible efficient electron injection.
- The TD-DFT calculations, at least TD-CAM-B3LYP/6-31G (d, p) was used to replicate the optical transitions in order to predict the excited and emission states; the predicted result of the absorption wavelengths for D1, D2, D3, D4, D5 and D6 is 805.02, 794.65, 801.53, 793.82, 790.72 and 727.01 nm respectively.

In summary, the decreasing of the band gap of these six dyes due to increasing the absorption wavelengths, then the best dye which can be used in photovoltaic cells such as donor of electronic in DSSCs, is one which has the small band gap, large wavelengths, appropriate FMO energy levels, higher LHE and ΔG^{inject}, and smallest λ_{total}, thus the all dyes Di (1 to 6) are appropriate to do this role.

Acknowledgements: This work was supported by Volubilis Program (N° MA/11/248), and the convention CNRST/CNRS (Project chimie 1009).

References

1. Mukhamed L. K., Dmitri Yu. Go., Alexei R. K., Tetsunari M., Hiroyuki F., Eisuke G., Junya H., Saki N., Susumu K., Tomoya H., Tsuyoshi M., *J. Poly. Science, part a: Poly. Chem.,* 53 (2015) 1067.

2. Nguyen V.C., Potje-Kamloth K., Thin Solid Films, 338 (1999) 142.
3. Li X.-G., Huang M R., Duan W., Yang Y. L., Chem. Rev. 102 (2002) 2925.
4. Wang G., Qian S., Xu J., Wang W., Liu X., Lu X., Li F., Physica Part B, 279(2000)116.
5. Chen H.Y., Hou J.H., Zhang S.Q., Liang Y.Y., Yang G.W., Yang Y., Yu L.P., Wu Y., Li G., Nat. Photonics, 3(2009) 649.
6. Zhang X., Jenekhe S. A., Macromolecules, 33(2000)2069.
7. Kulkarni A. P., Zhu Y., Jenekhe S. A., Macromolecules, 38(2005)1553.
8. Ego C., Marsitzky D., Becker S., Zhang J., Grimsdale A. C., Mullen K., MacKenzie J. D., Silva C., Friend R. H., J. Am. Chem. Soc., 125(2003)437.
9. Wu W.C., Liu C. L., Chen W. C., Polymer, 47(2006)527.
10. Thompson B. C., Madrigal L. G., Pinto M. R., Kang T. S., Schanze K. S., Reynolds J. R., J. Polym. Sci., Part A: Polym. Chem., 43(2005)1417.
11. Hancock J. M., Gifford A. P., Zhu Y., Lou Y., Jenekhe S. A., Chem. Mater., 18(2006)4924.
12. ChampionR. D., Cheng K. F., Pai, C. L., Chen W. C., Jenekhe S. A., Macromol. Rapid Commun., 26(2005)1835.
13. Babel A., Wind J. D., Jenekhe S. A., Adv. Funct. Mater., 14(2004)891.
14. Yamamoto T., Yasuda T., Sakai Y., Aramaki S., Macromol. Rapid Commun., 26(2005)1214.
15. Yamamoto T., Kokubo H., Kobashi M., Sakai Y., Chem. Mater., 16(2004)4616.
16. Chen M., Crispin X., Perzon E., Andersson M. R., Pullerits T., Andersson M., Inganas O., Berggren M., Appl. Phys. Lett., 87(2005)252105.
17. Yasuda T., Sakai Y., Aramaki S., Yamamoto T., Chem. Mater., 17(2005)6060.
18. Nalwa H.S., Editor, Handbook of Organic Conductive Molecules and Polymer, John Wiley, New York (1997)
19. Garnier F., Horowitz G., Peng X., Fichou D., Adv. Mater., 2(1990)562
20. Wang G., Qian S., Xu J., Wang W., Liu X., Lu X., Li F., Physica Part B, 279(2000)116
21. Ando S., Nishida J., Fujiwara E., Tada H., Inoue Y., Tokito S., Yamashita Y., Synth. Met., 156(2006)327
22. Demeter D., Roncali J., Jungsuttiwong S., Melchiorre F., Biagini P., Riccardo P., J. Mater. Chem. C, 2015, DOI: 10.1039/C5TC01183C
23. (a) Gadisa A., Svensson M., Andersson M.R., Inganas O., Appl. Phys. Lett., 84(2004)1609;
(b) Scharber M.C., Mühlbacher D., Koppe M., Denk P., Waldauf C., Heeger A.J., Brabec C.J., Adv. Mater., 18(2006)789;
(c) Brabec C.J., Cravino A., Meissner D., Sariciftci N.S., Fromherz T., Rispens M.T., Sanchez L., Hummelen J.C., Adv. Funct. Mater., 11(2001)374.
24. Yu J.-S.K., Chen W.-C., Yu C.-H., J. Phys. Chem. A, 107(2003)4268
25. Zhu Y., Champion R. D., Jenekhe S. A., Macromolecules, 39(2006)8712.
26. Sonmez G., Sonmez H. B., Shen C. K. F., Jost R. W., Rubin Y., Wudl F., Macromolecules, 38(2005)669.
27. (a)Becke A.D., J. Chem. Phys., 98(1993)5648.
(b) Ditchfield R., Hehre W.J., Pople J.A., J. Chem. Phys., 54(1971)724.
28. Magyar R.J., Tretiak S., J. Chem. Theory. Comput., 3(2007)976-987.
29. Yanai T., Tew D.P., Handy N.C., Chem. Phys. Lett., 393(2004)51.
30. Preat J., J. Phys. Chem. C, 114(2010)16.
31. Camino B., De-La-Pierre M., Ferrari A.M., J. Mol. Struct., 1046(2013)116.
32. Fitri A., Touimi Benjelloun A., Benzakour M., Mcharfi M., Hamidi M., Bouachrine M., Spectrochim. Acta A: Mol. Biomol. Spectrosc., 124(2014)646.
33. Fitri A., Touimi Benjelloun A., Benzakour M., Mcharfi M., Hamidi M., Bouachrine M., Spectrochim. Acta A: Mol. Biomol. Spectrosc., 132(2014)232.
34. Tomasi J., Mennucci B., Cammi R., Chem. Rev., 105(2005)2999.
35. Cossi M., Barone V., J. Chem. Phys., 115(2001)4708.

36. Adamo C., Barone V. A., Chem. Phys. Lett., 330(2000)152.
37. Frisch M.J., Trucks G.W., Schlegel H.B., Scuseria G.E., Robb M.A., Cheeseman J.R., Montgomery J.A., Vreven T., Kudin K.N., Burant J.C., Millam J.M., Iyengar S.S., Tomasi J., Barone V., Mennucci B., Cossi M., Scalmani G., Rega N., Petersson G.A., Nakatsuji H., Hada M., Ehara M., Toyota K., Fukuda R., Hasegawa J., Ishida M., Nakajima T., Honda Y., Kitao O., Nakai H., Klene M., Li X., Knox J.E., Hratchian H.P., Cross J.B., Bakken V., Adamo C., Jaramillo J., Gomperts R., Stratmann R.E., Yazyev O., Austin A.J., Cammi R., Pomelli C., Ochterski J.W., Ayala P.Y., Morokuma K., Voth G.A., Salvador P., Dannenberg J.J., Zakrzewski V.G., Dapprich S., Daniels A.D., Strain M.C., Farkas O., Malick D.K., Rabuck A.D., Raghavachari K., Foresman J.B., Ortiz J.V., Cui Q., Baboul A.G., Clifford S., Cioslowski J., Stefanov B.B., Liu G., Liashenko A., Piskorz P., Komaromi I., Martin R.L., Fox D.J., Keith T., Laham A.M.A., Peng C.Y., Nanayakkara A., Challacombe M., Gill P.M.W., Johnson B., Chen W., Wong M.W., Gonzalez C., Pople J.A., Gaussian 09, Revision A02, Gaussian Inc, Wallingford CT, (2009).
38. Akoudad S., Roncali J., Synth Met., 101(1999)149.
39. Pepitone M. F., Hardaker S.S., Gregory R.V., Chem. Mater., 15(2003)557.
40. Yakhanthip T., Jungsuttiwong S., Namuangruk S., Kungwan N., Promarak V., Sudyoadsuk T., et al., J. Comput. Chem., 32(2011)1568.
41. Asbury J.B., Wang Y.Q., Hao E., Ghosh H., Lian T., Res. Chem. Intermed., 27(2001)393.
42. Sang–aroon W., Saekow S., Amornkitbamrung V., J. Photochem. Photobiol. A, 236(2012)35.
43. Qin C., Clark A.E., Chem. Phys. Lett., 438(2007)26.
44. Zhang Z.L., Zou L.Y., Ren A.M., Liu Y.F., Feng J.K., Sun C.C., Dyes Pigm., 96(2013)349.
45. Asbury J.B., Wang Y.Q., Hao E., Ghosh H., Lian T., Res. Chem. Intermed., 27(2001)393.
46. Preat J., Jacquemin D., Michaux C., Perpète E.A., Chem. Phys., 376(2010)56.
47. Zhang J., Li H.B., Sun S.L., Geng Y., Wu Y., Su Z.M., J. Mater Chem., 22(2012)568.
48. Zhang J., Kan Y.H., Li H.B., Geng Y., Wu Y., Su Z.M., Dyes Pigm., 95(2012)313.
49. Ding W.L., Wang D.M., Geng Z.Y., Zhao X.L., Xu W.B., Dyes Pigm., 98(2013)125.
50. Sang–aroon W., Saekow S., Amornkitbamrung V., J. Photochem. Photobiol. A, 236(2012)35.
51. Koopmans T. A., Physica, 1(1933)104.
52. Balanay M.P., Kim D.H., J. Mol. Struct. Theochem, 910(2009)20.
53. Vasudevan J., Stibrany R.T., Bumby J., Knapp S., Potenza J.A., Emge T.J., Schugar H.J., J. Am. Chem. Soc., 118 (1996) 11676.
54. Scheer H., Inhoffen H.H., in: D. Dolphin (Ed.), The Porphyrins, Academic, New York, 1978.
55. Tawada Y., Tsuneda T., Yanagisawa S., Yanai T., Hirao K., J. Chem. Phys., 120 (2004) 8425.
56. Yu J. S. K., Chen W. C., Yu C. H., J. Phys. Chem. A., 107 (2003) 4268.
57. Azazi A., Mabrouk A., Alimi K., Comput. Theoret. Chem., 978 (2011) 7.